RESEARCH ARTICLE

Single-Molecule Conductance of 1,4-Azaborine Derivatives as Models of BN-doped PAHs

Lucía Palomino-Ruiz,[a],[b] Sandra Rodríguez-González,[c],‡ Joel G. Fallaque,[b] Irene R. Márquez,[a],[d] Nicolás Agraït,[b],[e],[f] Cristina Díaz,[c],‖ Edmund Leary,[b] Juan M. Cuerva,[a] Araceli G. Campaña,[a] Fernando Martín,*[b],[c],[f] Alba Millán,*[a] M. Teresa González*[b]

This work is dedicated to the memory of Prof. Kilian Muñiz.

[a] L. Palomino-Ruiz, Dr. I. R. Márquez, Prof. Dr. J. M. Cuerva, Dr. A. G. Campaña, Dr. A. Millán
Departamento de Química Orgánica, Facultad de Ciencias
Unidad de Excelencia de Química Aplicada a Biomedicina y Medioambiente (UEQ)
Universidad de Granada, 18071 Granada, Spain
E-mail: amillan@ugr.es
[b] L. Palomino-Ruiz, J. G. Fallaque, Prof. Dr. N. Agraït, Dr. E. Leary, Prof. Dr. F. Martín, Dr. M. T. González
Fundación IMDEA Nanociencia, 28049 Madrid, Spain
E-mail: fernando.martin@uam.es
E-mail: teresa.gonzalez@imdea.org
[c] Dr. S. Rodríguez-González, Dr. C. Díaz, Prof. Dr. F. Martín
Departamento de Química, Módulo 13
Universidad Autónoma de Madrid, 28049 Madrid, Spain
[d] Dr. I. R. Márquez
Centro de Instrumentación Científica
Universidad de Granada, 18071 Granada, Spain
[e] Prof. Dr. N. Agraït
Departamento de Física de la Materia Condensada
Universidad Autónoma de Madrid, 28049, Madrid, Spain
[f] Prof. Dr. N. Agraït, Prof. Dr. F. Martín
Condensed Matter Physics Center (IFIMAC)
Universidad Autónoma de Madrid, 28049 Madrid, Spain
‡ Dr. S. Rodríguez-González
Present address
Departamento de Química Física, Facultad de Ciencias
Universidad de Málaga, 29071, Málaga, Spain.
‖ Dr. C. Díaz
Present address
Departamento de Química Física, Facultad de CC. Químicas
Universidad Complutense de Madrid, 28040 Madrid, Spain.

Supporting information for this article is given via a link at the end of the document.

Abstract: The single–molecule conductance of a series of BN-acene-like derivatives has been measured by using scanning tunneling break-junction techniques. A strategic design of the target molecules has allowed us to include azaborine units in positions that unambiguously ensure electron transport through both heteroatoms, which is relevant for the development of customized BN-doped nanographenes. We show that the conductance of the anthracene azaborine derivative is comparable to that of the pristine all-carbon anthracene compound. Notably, this heteroatom substitution has also allowed us to perform similar measurements on the corresponding pentacene-like compound, which is found to have a similar conductance, thus evidencing that B–N doping could also be used to stabilize and characterize larger acenes for molecular electronics applications. Our conclusions are supported by state-of-the-art transport calculations.

Introduction

The tailored inclusion of heteroatoms in polycyclic aromatic hydrocarbons (PAHs) is a widely used approach to modify the physico-chemical properties of the parent structures.[1] In particular, heteroatom-doped π-systems are of interest in molecular electronics, as they can be used to modulate the electronic transport properties of organic frameworks.[2] They can also be used as models for extended 2D-analogues, *e.g.*, doped graphene.[3] So, establishing direct correlations between the structure of doped-PAHs and charge transport properties is essential for the application of these materials in molecular electronics.

Investigations of the electronic transport in such systems at the single-molecule level are properly carried out by means of break-junction techniques.[4] In most reported studies, heteroatoms have been placed laterally or as side groups for synthetic ease, so that electronic transport takes place through the eigenchannels already accessible in the pristine all-carbon analogues. In this context, molecules containing oxygen, sulphur, boron, phosphorous, nitrogen or silicon, among others, have been

experimentally studied.[5,6] However, little is known about the situation when electrons are forced to pass directly through heteroatoms, placed along the most favourable path.

There are a few known examples in which electrons have been forced to pass through heteroatoms,[5c,6a,7,8] e.g., molecular wires with π-σ-π backbones, where the σ moiety is a single heteroatom[7] or a sequence of them,[8] and no heteroatom is embedded in the aromatic system. These studies have shown that heteroatoms can impact the electron transfer due to their difference in size, polarizability or electronegativity with respect to carbon atoms. However, in some cases, it is difficult (sometimes even impossible) to build all-carbon references to quantify the effect of heteroatoms sitting in the transport pathway.

To assess the effect of the heteroatoms unambiguously on the electronic transport through PAHs or 2D analogues, the experimental approach should ideally meet the following three criteria: i) heteroatoms should be embedded in the π-core; ii) electrons should unequivocally pass through the heteroatoms, and iii) comparison with the corresponding all-carbon analogues should be possible. To meet these criteria, in this work we have focussed on azaborine derivatives.[9] The simplest azaborine is an isoster of benzene where a C=C moiety has been replaced by a B-N unit (Figure 1a). In this case, two electrons provided by the nitrogen atom compensate the electron deficiency at the boron. This electron donation promotes a unique polarization in the aromatic ring[9a] thus affecting its stability and aromatic character.[10,11] Azaborines are also perfect candidates to be embedded in the core of nanographenes, since they maintain the original topology. Consequently, they have been widely used as models of BN-doped nanostructures.[12,13] In this respect, a very recent single-molecule conductance study on a BN-substituted phenanthrene derivative has shown a slight increase of conductance with respect to its all-carbon analogue,[14] which makes this molecule potentially interesting for organic electronics. Nevertheless, the studied molecule was a 1,2-azaborine derivative, in which the BN-moiety was located at the edge of the π scaffold, thus constituting another example of the indirect influence of the heteroatoms on the electronic transport. In contrast, in 1,4-azaborines, the heteroatoms are placed in *para* position, which, joined to a strategic location of the linking groups, unequivocally ensures that the electron pathway goes through the B and N atoms embedded in a fully conjugated ring. Moreover, this atom distribution favours a directional π-electron delocalisation rather than a cyclic one, thus reducing the aromaticity. For this reason, 1,4-azaborines have been considered as push-pull π-electron systems rather than π-aromatic molecules.[11] To the best of our knowledge, the manner in which this charge distribution affects the conductance has never been studied.

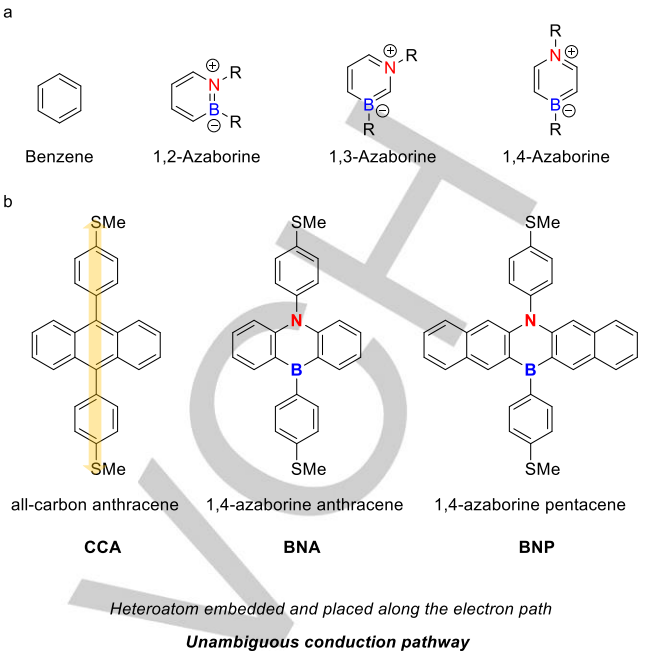

Figure 1. (a) CC/BN isosterism; (b) Structures of the synthesized molecules.

In this work, we have performed single-molecule conductance studies of the compounds shown and denoted in Figure 1b, namely the all-carbon anthracene derivative **CCA**, its corresponding 1,4-azaborine isoster **BNA**, and the more extended 1,4-azaborine pentacene derivative **BNP**, to quantify the effect of the 1,4 boron-nitrogen substitution on the electronic transport unambiguously. These compounds include thiomethyl (SMe) phenyl linkers, which are well-known to provide a good contact with metallic electrodes in break-junction experiments,[15] and avoid known issues with thiolate groups.[16] This is essential for a quantitative comparison between the three systems. The placement of the linkers in *para* positions ensures that electron conduction is forced through the heteroatoms. We show that the conductance of the 1,4-azaborine derivative **BNA** is comparable to that of the pristine **CCA** compound. Remarkably, this heteroatom substitution allows us to perform measurements on the pentacene-like **BNP** compound, which is very unstable in its all-carbon form,[17] evidencing that B–N isosterism could be a plausible strategy to stabilize larger acenes for optoelectronic applications.[13e] Our findings are supported by state-of-the-art transport calculations, which also show that the small differences in conductance found for the three systems are related to differences in aromaticity.

Results and Discussion

Synthesis of target molecules

CCA, **BNA** and **BNP** bearing suitable Au-anchoring groups (SMe) were prepared *via* the following procedures. **CCA** was synthesized by a double Suzuki cross-coupling reaction of 9,10-dibromoanthracene and (4-(methylthio)phenyl)boronic acid. **BNA** and **BNP** were obtained by Buchwald-Hartwig cross-coupling reactions of the corresponding haloarenes and 4-

(methylthio)aniline, followed by a challenging final lithiation-boration sequence, which required careful optimization. For further details of synthesis, see the Supporting Information.

Anthracene derivatives with and without 1,4 azaborine substitution

Single-molecule conductance (*G*) experiments were carried using the scanning tunnelling microscope break-junction (STM-BJ) technique (See the Supporting Information for further details). The experiments are based on a push-pull process between the STM tip and the substrate. During the pulling, *G* decreases with the distance between electrodes (*z*), displaying plateaus at $G<G_0$ ($G_0 = 2e^2/h$) if molecular bridges have been formed between tip and substrate. When building 1D *G* histograms or 2D *G*-*z* histograms with thousands of these *G* vs *z* traces, a peak or a cloud is formed in the regions where plateaus repeatedly appear, signaling the characteristic molecular-junction conductance and stretching length.

We start comparing compounds **CCA** and **BNA**, which differ structurally only in the 1,4 azaborine central substitution. Their 2D histograms are shown in Figures 2a and 2b, respectively. They show a similar shape, with a broad and sloping conductance signal located between $\log(G/G_0) = -5$ and -6 for both, with a modest shift towards lower values for **BNA**. This sloping profile, already observed in other structures,[18] is probably due to a significant interaction between the central part of the molecules and the gold electrodes as the molecules slide over them during the pulling process. This interaction seems to be favoured by the acene motif. The sloping clouds of the 2D histograms translate into asymmetric peaks in the corresponding 1D histograms, which are superimposed in Figure 2c for a better comparison. Therefore, to determine the main conductance value for each compound properly, we first separated the traces with the flatter plateaus, where the interaction of gold with the central part of the molecules should be less important, following an unsupervised k-means clustering subdivision similar to that found in the literature[19] (see details in the Supporting Information). By fitting a gaussian to the conductance peaks in the corresponding 1D histograms, we determine the conductance of the compounds to be $\log(G/G_0) = -5.3 \pm 0.31$ for **CCA**, and -5.6 ± 0.33 for **BNA**. These values are marked by short vertical lines over the histograms in Figure 2c. Higher conductance plateaus were also revealed in the clustering process, which will be discussed later. The analysis of the plateau-length (Δz) distributions included as inset in Figure 2c demonstrates that, for both molecules, the end of the Gaussian distribution concurs with the expected sulfur-to-sulfur (S-S) molecular distance (1.48 nm), once an interval of 0.4 nm is subtracted to compensate for the electrode retraction after the gold contact breaks (vertical grey line in the figure, see Supporting Information for details). We conclude therefore that equivalent molecular junctions are being formed for both compounds, with molecules fully extended between the gold electrodes. Importantly, the 1,4-BN substitution in the central ring not only permits the electron transport through the molecule, but also leads to a molecular conductance of the same order of magnitude as that of the all-carbon structure.

We observe nevertheless that the conductance of both compounds is nearly two orders of magnitude smaller than that of the *p*-terphenyl derivative equivalent of **CCA** (4,4''-bis(methylthio)-1,1':4',1''-terphenyl).[20] A full comparison with this reference compound is included in the Supporting Information (Figures S1 and S2) for completeness. Most likely, this difference is due to the increased average torsion angle between the outer phenyl rings and the central group.[21] Indeed, for *p*-terphenyl the inter-ring angle leading to the minimum energy is 33.8 degrees, while for CCA it is 70 degrees, according to our theoretical calculations (see below and table S1). This observation is compatible with previous conductance measurements for benzene and naphthalene diamine analogues to **CCA**.[21b,22]

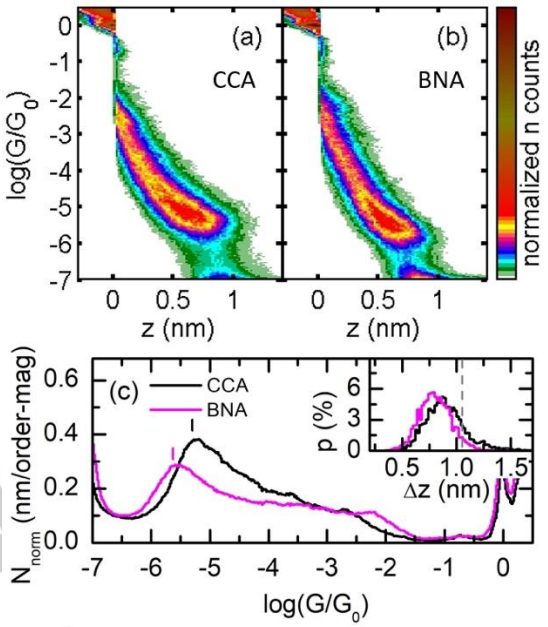

Figure 2. (a and b) 2D histograms for compounds **CCA** and **BNA**, respectively, build from all traces displaying plateaus. (c) Corresponding 1D histograms for **CCA** and **BNA**. The inset shows their plateau-length distribution, where the grey line corresponds to the molecular S-S distance minus 0.4 nm, accounting for gold retraction.

1,4-BN substitution in larger acenes

Considering that BN-doping seems to involve a minimum decrease of the conductance with respect to the pristine structures, we hypothesized that 1,4-azaborine substitution could be a route for investigating single-molecule conductance of structures that, in their all-C version, would be extremely challenging, if not impossible. This is the case of larger acenes, which have raised high interest in organic electronics due to their high charge-carrier mobility,[23] but whose instability in solution[24] precludes the isolation and their potential implementation in single-molecule devices. For example, for 6,13-diphenylpentacene, the pentacene analogue of **CCA**, a lifetime in the presence of oxygen and light of only 8.5 minutes in CH_2Cl_2 solution has been reported in the literature.[17] Although there is no consensus towards the origin of such instability, the reason seems to be related with the increasing biradical character of the ground states of acenes as their size increases.[25] In this sense, as azaborines do not present a quasi-degenerate ground state,[11] the BN/CC isosterism could lead to structures that are stable enough[13e,26] to investigate their electron transport properties under ambient conditions.

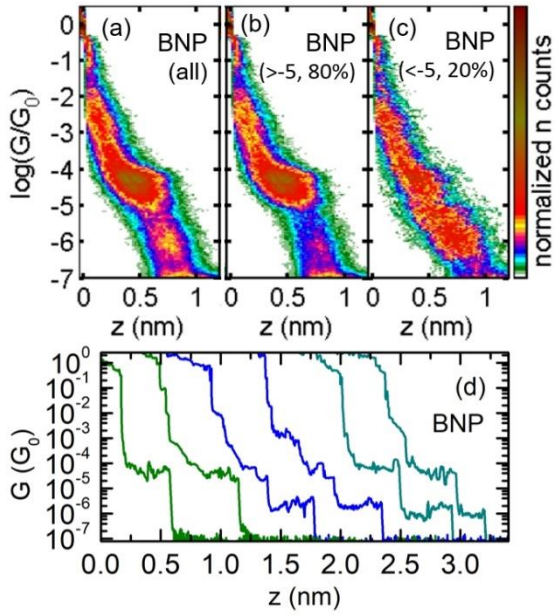

Figure 3. (a) 2D histogram for compound **BNP**. (b) and (c) Independent 2D histograms of two separated groups for BNP: traces without and with plateaus below log(G/G0) = –5, respectively. (d) Representative individual raw conductance traces displaying clear plateaus only above log(G/G0) = –5 (green), only below log(G/G0) = –5 (blue) and in both regions (cyan). The first two traces contribute to the histogram of part (b), while the last four contribute to that of part (c).

Figure 3a shows the 2D histogram obtained for **BNP** from nearly two thousand *G*-*z* traces with plateaus. This histogram displays a well-defined flat cloud of high conductance at around log(G/G_0) = –4.5, which clearly extends to distances shorter than for the previous compounds. This short plateau length suggests that it does not result from a linker-to-linker configuration. In addition, the histogram displays a less clear conductance cloud below log(G/G_0) = –5. A better assessment of the latter could be achieved by a simple search for traces with plateaus in this region (identical to that performed in the whole conductance range for previous histograms). The independent 2D histograms for traces without and with plateaus below log(G/G_0) = –5 are shown in Figure 3b and 3c, while different raw individual traces for **BNP** are displayed in Figure 3d, showing clear plateaus in both conductance ranges. The corresponding 1D histograms can be found in Figure 4a.

The comparison of the clustering subdivision for **BNP** with that previously described for **CCA** and **BNA** (see Supporting Information) shows that the dominant **BNP** high-conductance signal is identical to that present (although much less apparent) in **CCA** and **BNA** (see Figures S3 and S4). In addition, this signal is also the same as that observed in a modified compound including a linking group at only one of its ends, **BNA-1-linker** (see Figure S6). These results suggest that the direct interaction of the electrodes with the central acene unit is at the origin of the observed high-conductance plateaus. While this interaction mainly leads to sloping plateaus in **CCA** and **BNA**, with only occasional flat high-conductance plateaus, the stronger interation of the pentacene unit in **BNP** with gold, due to its larger electron density, leads to flat plateaus in most cases. This direct interaction of the acene with gold has been reported to translate in an increasing difficulty to form end-to-end junctions as the acene length increases.[27] The fact that no differences between **CCA** and **BNA** are observed in the high-conductance plateaus indicates that the whole acene is participating in the attachment, with no specific contribution of B or N. Figure 4b and 4c show the plateau length distributions of plateaus above and below log(G/G_0) = –5, reinforcing their common origin in all studied compounds. The presence of π-π stacked molecules between the electrodes should result in longer (or at least similarly long) junctions than in the single-molecule case, depending on the overlapping configuration.[28] While these might be occurring here, contributing to the sloping plateaus described in the previous section or even being undetected if their conductance is too low, they would not account for the observed high-conductance plateaus, since they are significantly shorter in length.

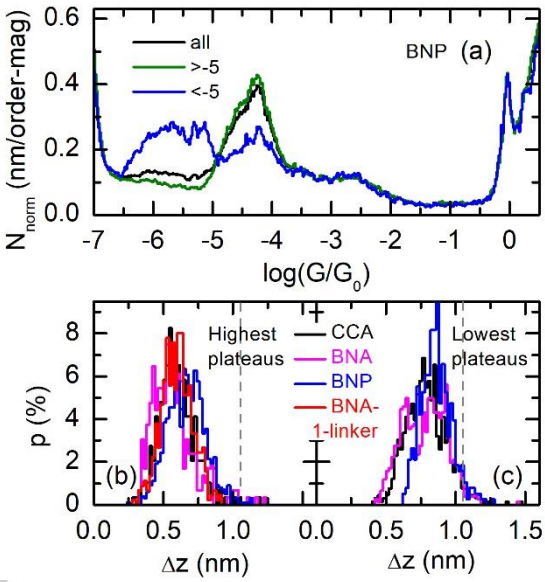

Figure 4. (a) 1D histograms for all traces of **BNP** (black), and those of Figure3b (green) and 3c (blue). (b) and (c) plateau-length distribution for plateaus above and below log (G/G_0) = –5, respectively, for all the studied compounds, separated using a clustering subdivision (see main text). Plateaus above log(G/G_0) = –5 are around 0.2 nm shorter that those below. The grey line corresponds to the expected length of plateaus for the S-S molecular distance.

The lower conductance signal for **BNP** constitutes only 20% of the total traces; however, both the conductance and the plateau length are in the range of those of **CCA** and **BNA**. We therefore assign this set of plateaus to **BNP** molecular junctions with the molecule fully extended between the electrodes. We determine its typical conductance to be log(G/G_0) = –5.9 ± 0.40 (see Figure S4c in the Supporting Information). This result demonstrates that the lateral extension of the central acene has little effect in the fully extended molecular junction conductance.

Theoretical modelling

In order to rationalize these experimental results, we have performed first-principles conductance simulations of the single-molecule **CCA**, **BNA**, and **BNP** junctions. We have employed the TranSIESTA/TBTrans set of codes, based on the combination of DFT and non-equilibrium Green's functions (NEGFs),[29] together with optimized geometries using VASP.[30] In particular, following the state of the art, zero-bias self-energy corrected density functional theory (DFT+Σ method),[31] was used to overcome the

shortcomings of standard DFT in providing accurate energy positions of molecular states with respect to the junction Fermi level.

Molecules were placed fully extended in between two Au (111) electrodes with asymmetric interfaces, thereby simulating the Au STM tip and the non-planar surface in the STM-BJ measurements. Therefore, as BN and NB polarizations of the molecule with respect to the junction are equally probable in the experiment, we have considered both tip-N-B-substrate (T-N-B-S) and tip-B-N-substrate (T-B-N-S) orientations (see Figure S12 in the Supporting Information).

The calculated DFT+Σ zero-bias transmission functions for the above three compounds in the T-N-B-S scenario are shown in Figure 5. Results for the other polarization direction are shown in Figure S14 of the Supporting Information and are compatible with the ones shown here. As expected, the transmission probability is highest at the energies of the molecular levels, namely, those corresponding to the occupied (peaks at negative $E-E_F$) and unoccupied (peaks at positive $E-E_F$) states. However, these resonances are so far from the Fermi level ($E-E_F=0$) that they do not lie within the energy window that is experimentally accessible with the applied bias voltage.

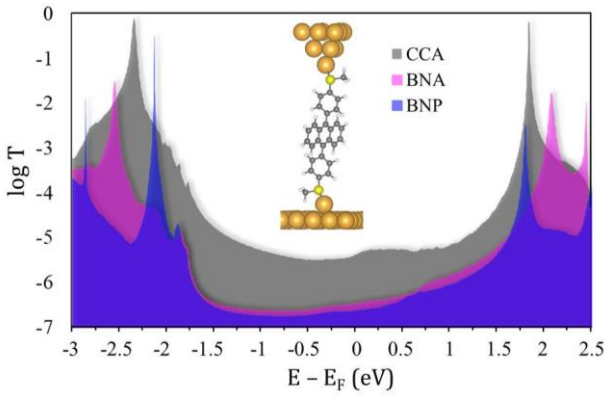

Figure 5. Calculated DFT+Σ zero bias transmission as a function of the energy for compounds: **CCA** (grey), **BNA** (pink), and **BNP** (blue), in the T-N-B-S polarization scenario. Inset: The molecular junction containing the **CCA** molecule (H, white; C, gray; S: yellow; and Au: gold).

Thus, the computed transmission spectra reveal that the low-bias conductance occurs through a non-resonant tunnelling process, dominated by a transmission function that varies smoothly around the Fermi level. This effect is the result of the appearance of the so-called mid-gap states arising from the interaction between the undercoordinated Au adatom, the substrate and the molecule, involving the sulfur anchors (see Figure S15 in the Supporting Information).[32] In these cases, the zero-bias conductance can be evaluated by the transmission at the Fermi level, within the Landauer approach, $G/G_0 = T(E_F)$.

As can be seen in Table 1, for both T-N-B-S and T-B-N-S scenarios, the calculated conductance values follow the experimental trend, according to which the BN substitution reduces the conductance, and this does not depend on either the length of the central azaborine derivative or the polarization direction. The same qualitative trend was found without including the self-energy correction Σ to the calculated transmission functions (see Table S2 in the Supporting Information).

Quantitative differences with the experimental values are likely due to the fact that the calculated conductance values have been obtained for the fully relaxed (energetically most stable) junction (which is mandatory for a direct comparison between the three systems), while the measured value for each single trace corresponds to an average structure representing the thermal structural fluctuations suffered by the molecule during the experiment. This fact is more evident in molecules with internal dihedral degrees of freedom, as is the case for the studied molecules.[21b]

Table 1. Calculated DFT+Σ zero bias and experimentally measured conductance values ($\log(G/G_0)$) in the single molecule-junctions, and NICS (1.7)zz indexes for the central ring (in ppm) for **CCA**, **BNA** and **BNP**. Values for the (T-B-N-S) polarization are in parentheses.

Compound	*CCA*	*BNA*	*BNP*
$log(G/G_0)_{DFT+\Sigma}$	-5.39	-6.46 (-6.30)	-6.62 (-6.45)
$log(G/G_0)_{exp.}$	-5.30± 0.31	-5.60 ± 0.33	-5.90 ± 0.40
NICS(1.7)zz	-24.53	-12.21(-12.35)	-8.61 (-8.28)

As mentioned in the introduction, BN substitution promotes a polarization into the aromatic ring which could translate in a diode effect with currents flowing more easily in one direction of the molecule than in the other and, hence, in asymmetric current vs voltage (*I-V*) curves. To test this hypothesis, we have repeated our break-junction experiment for **BNA** recording a series of *I-V* curves along the conductance plateaus between +1 and -1 V (see details and final *I-V* curves in the Supporting Information, Figures S7 and S8). We observed only a small effect, with an average rectification ratio (ratio between the higher and lower currents recorded at oppositive voltages, here ±1 V) of 1.8 ± 0.7, in rather linear *I-V* curves. This ratio is only slightly larger than that previously reported for fully symmetric compounds,[5b,33] and similar to that observed in N-phenylbenzamide derivatives,[34] where the dependence of the rectification factor with the strength of the molecule's linking group is demonstrated. This result is consistent with the transmission curves displayed in Figure 5, with the gold Fermi level being practically at the center of a wide HOMO-LUMO gap.

Given the controversy about the effect of aromaticity in the electronic properties at the single-molecule level,[35] an effort has been made to understand and quantify the role of this parameter in the conductance values for these compounds. We have calculated the Nucleus-Independent Chemical shift (NICS) index[36] for each individual fused ring in **CCA**, **BNA** and **BNP** molecules. Only out-of-plane contributions were evaluated, namely at 1.7 Å above the molecular plane, NICS (1.7)zz, which has been established as the optimal height where the π-contributions are of interest (σ-only method)[37] (see the Supporting Information for further details). The results, reported in Table 1, show that the central ring, through which conductance mainly takes place, suffers a considerable loss of aromaticity after BN-substitution in **CCA**, which in these compounds reflects a conjugation reduction. Similarly, a slight decrease in aromaticity is observed when going from **BNA** to **BNP**. Therefore, we conclude that, in this kind of compound, the higher the aromaticity the higher the conductance.

To check how much of the observed changes in conductance for these compounds is due to changes in aromaticity or just to conformational modifications induced by the BN-substitution on the dihedral angle between the linker ring and the central acene, we have performed additional calculations in which the aforementioned angle in BN-substituted species is set to be identical to that of the all-carbon species. This is a relevant question since the corresponding dihedral angles are quite different: around 90º (Nitrogen side) and 54º (Boron side) in **BNA** and **BNP** vs. 70º in **CCA** (see Supporting Information, *Computational calculations and discussion* section). The results, given in the Supporting Information (Table S2), show that approximately half of the difference in the logarithm of the conductance between **CCA** and the BN-doped compounds can be accounted for by the angle variation, while the general conductance variation trend still remains, supporting the importance of the aromaticity in these compounds.

Conclusion

We have performed single-molecule conductance measurements of BN-doped anthracene and pentacene molecules in positions that ensure an unequivocal electron pathway through the heteroatoms. We have shown that the 1,4-BN-doping permits the electron transport through the molecules, giving rise to conductance values of the same order of magnitude as those of the pristine scaffolds. These findings are supported by state-of-the-art transport calculations, which point to the loss of aromaticity due to the BN-substitution as the reason for the slight conductance decrease. They also show that the above conclusions are independent of the B-N polarization direction in the molecular junction. Importantly, this heteroatom substitution pattern has enabled us to measure conductance in a pentacene-like core, supporting that CC/BN isosterism could be a plausible strategy to stabilize and characterize larger acenes, which can be relevant for charge transfer studies and optoelectronics applications involving large acene compounds.

Acknowledgements

This work has been supported by the MICINN projects PID2019-105458RB-I00, PID2019-106732GB-I00, PGC2018-101873-A-I00, CTQ2017-85454-C2-1-P, FIS2016-77889-R and MAT2017-88693-R, the European Research Council (ERC) (677023), the FEDER/Junta de Andalucía project A-FQM-221-UGR18 and the Comunidad de Madrid project NanoMagCOST (CM S2018/NMT-4321). We also thank Severo Ochoa Programme for Center of Excellence in R&D (SEV-2016-0686) and María de Maeztu Programme for Units of Excellence in R&D (CEX2018-000805-M). We acknowledge the allocation of computer time by the Red Española de Supercomputación and the Centro de Computación Científica at the Universidad Autónoma de Madrid (CCC-UAM). J.G.F. thanks the PFI program of the MICINN co-financed by the European Social Fund. I.R.M. thanks MICINN for a Personal Técnico de Apoyo contract (PTA2017-13681-I). E.L. thanks the Comunidad de Madrid grant Atracción de Talento 2019-T1/IND-16384.

Keywords: molecular electronics • single-molecule studies • nanotechnology • azaborine • break junction technique • density functional calculations • polycyclic aromatic hydrocarbons

[1] a) X. Y. Wang, X. Yao, A. Narita, K. Müllen, *Acc. Chem. Res.* **2019**, *52*, 2491-2505; b) M. Stępień, E. Gońka, M. Żyła, N. Sprutta, *Chem. Rev.* **2017**, *117*, 3479-3716.

[2] a) A. Staykov, X. Li, Y. Tsuji, K. Yoshizawa, *J. Phys. Chem. C* **2012**, *116*, 18451-18459; b) W. Zhang, Y. Liu, G. Yu, *Adv. Mater.* **2014**, *26*, 6898-6904.

[3] a) M. Pumera *J. Mater. Chem. C* **2014**, *2*, 6454-6461. b) T. Granzier-Nakajima, K. Fujisawa, V. Anil, M. Terrones, Y.-T. Yeh, *Nanomaterials* **2019**, *9*, 425; c) S. Kawai, S. Nakatsuka, T. Hatakeyama, R. Pawlak, T. Meier, J. Tracey, E. Meyer, A. S. Foster, *Sci. Adv*. **2018**, *4*, eaar7181.

[4] a) M. A. Reed, C. Zhou, C. J. Muller, T. P. Burgin, J. M. Tour, *Science* **1997**, *278*, 252-254; b) N. Agraït, A. Yeyati, J. van Ruitenbeek, *Phys. Rep.* **2003**, *377*, 81-279; c) B. Xu, N. J. Tao, *Science* **2003**, *301*, 1221-1223.

[5] Representative example for single type of heteroatom: a) R. S. Klausen, J. R. Widawsky, T. A. Su, H. Li, Q. Chen, M. L. Steigerwald, L. Venkataraman, C. Nuckolls, *Chem. Sci.* **2014**, *5*, 1561-1564; b) W. Chen, H. Li, J. R. Widawsky, C. Appayee, L. Venkataraman, R. Breslow, *J. Am. Chem. Soc.* **2014**, *136*, 918-920; c) D. Miguel, L. Álvarez de Cienfuegos, A. Martin-Lasanta, S. P. Morcillo, L. A. Zotti, E. Leary, M. Burkle, Y. Asai, R. Jurado, D. J. Cárdenas, G. Rubio-Bollinger, N. Agraït, J. M. Cuerva, M. T. Gonzalez, *J. Am. Chem. Soc.* **2015**, *137*, 13818-13826; d) E. J. Dell, B. Capozzi, J. Xia, L. Venkataraman, L. M. Campos, *Nat. Chem.* **2015**, *7*, 209-214; e) Z. Cai, W.-Y. Lo, T. Zheng, L. Li, N. Zhang, Y. Hu, L. Yu, *J. Am. Chem. Soc.* **2016**, *138*, 10630-10635; f) A. K. Ismael, K. Wang, A. Vezzoli, M. K. Al-Khaykanee, H. E. Gallagher, I. M. Grace, C. J. Lambert, B. Xu, R. J. Nichols, S. J. Higgins, *Angew. Chem. Int. Ed.* **2017**, *56*, 15378-15382; *Angew. Chem.* **2017**, *129*, 15580-15584; g) Y. Yang, M. Gantenbein, A. Alqorashi, J. Wei, S. Sangtarash, D. Hu, H. Sadeghi, R. Zhang, J. Pi, L. Chen, X. Huang, R. Li, J. Liu, J. Shi, W. Hong, C. J. Lambert, M. R. Bryce, *J. Phys. Chem. C* **2018**, 122, 14965-14970; h) X. Liu, X. Li, S. Sangtarash, H. Sadeghi, S. Decurtins, R. Häner, W. Hong, C. J. Lambert, S.-X. Liu, *Nanoscale* **2018**, *10*, 18131-18134.

[6] Representative example for multiple heteroatoms: a) L. J. O'Driscoll, J. M. Hamill, I. Grace, B. W. Nielsen, E. Almutib, Y. Fu, W. Hong, C. J. Lambert, J. O. Jeppesen, *Chem. Sci.* **2017**, *8*, 6123-6130; b) M. Baghernejad, C. Van Dyck, J. Bergfield, D. R. Levine, A. Gubicza, J. D. Tovar, M. Calame, P. Broekmann, W. Hong, *Chem. Eur. J.* **2019**, *25*, 15141-15146; c) A. Markin, A. K. Ismael, R. J. Davidson, D. C. Milan, R. J. Nichols, S. J. Higgins, C. J. Lambert, Y.-T. Hsu, D. S. Yufit, A. Beeby, *J. Phys. Chem. C* **2020**, *124*, 6479-6485.

[7] Y.-H. Wang, H. Huang, Z. Yu, J.-F. Zheng, Y. Shao, X.-S. Zhou, J.-Z. Chen, J.-F. Li, *J. Mat. Chem. C* **2020**, *8*, 6826-6831.

[8] T. A. Su, H. Li, R. S. Klausen, J. R. Widawsky, A. Batra, M. L. Steigerwald, L. Venkataraman, C. Nuckolls, *J. Am. Chem. Soc.* **2016**, *138*, 7791-7795.

[9] Reviews: a) P. G. Campbell, A. J. V. Marwitz, S. Y. Liu, *Angew. Chem. Int. Ed.* **2012**, *51*, 6074-6092; *Angew. Chem.* **2012**, *124*, 6178-6197; b) G. Bélanger-Chabot, H. Braunschweig, D. K. Roy, *Eur. J. Inorg. Chem.* **2017**, 4353-4368; c) Z. X. Giustra, S.-Y. Liu, *J. Am. Chem. Soc.* **2018**, *140*, 1184-1194.

[10] M. Kranz, T. Clark, *J. Org. Chem.* **1992**, *57*, 5492-5500.

[11] M. Baranac-Stojanović, *Chem. Eur. J.* **2014**, *20*, 16558-16565.

[12] Reviews: a) X. Y. Wang, J. Y. Wang, J. Pei, *Chem. Eur. J.* **2015**, *21*, 3528-3539; b) J. Huang, Y. Li, *Front. Chem.* **2018**, *6*, 341.

[13] Recent examples: a) K. Matsui, S. Oda, K. Yoshiura, K. Nakajima, N. Yasuda, T. Hatakeyama, *J. Am. Chem. Soc.* **2018**, *140*, 1195-1198; b) D. T. Yang, T. Nakamura, Z. He, X. Wang, A. Wakamiya, T. Peng, S. Wang, *Org. Lett.* **2018**, *20*, 6741-6745; c) S. Nakatsuka, N. Yasuda, T. Hatakeyama, *J. Am. Chem. Soc.* **2018**, *140*, 13562-13565; d) J. S. A. Ishibashi, C. Darrigan, A. Chrostowska, B. Li, S. Y. Liu, *Dalton Trans.* **2019**, *48*, 2807-2812; e) F.-D. Zhuang, Z.-H. Sun, Z.-F. Yao, Q.-R. Chen, Z. Huang, J.-H. Yang, J.-Y. Wang, J. Pei, *Angew. Chem. Int. Ed.* **2019**, *58*, 10708-10712; *Angew. Chem.* **2019**, *131*, 10818-10822; f) J. Dosso,

T. Battisti, B. W. Ward, N. Demitri, C. E. Hughes, P. A. Williams, K. D. M. Harris, D. Bonifazi, *Chem. Eur. J.* **2020**, *26*, 6608-6621.

[14] Z.-H. Zhao, L. Wang, S. Li, W.-D. Zhang, G. He, D. Wang, S.-M. Hou, L.-J. Wan, *J. Am. Chem. Soc.* **2020**, *142*, 8068-8073.

[15] a) Y. S. Park, A. C. Whalley, M. Kamenetska, M. L. Steigerwald, M. S. Hybertsen, C. Nuckolls, L. Venkataraman, *J. Am. Chem. Soc.* **2007**, *129*, 15768-15769; b) M. Frei, S. V. Aradhya, M. S. Hybertsen, L. Venkataraman, *J. Am. Chem. Soc.* **2012**, *134*, 4003-4006.

[16] E. Leary, L. A. Zotti, D. Miguel, I. R. Márquez, L. Palomino-Ruiz, J. M. Cuerva, G. Rubio-Bollinger, M. T. González, N. Agraït, *J. Phys. Chem. C* **2018**, *122*, 3211- 3218.

[17] I. Kaur, W. Jia, R. P. Kopreski, S. Selvarasah, M. R. Dokmeci, C. Pramanik, N. E. McGruer, G. P. Miller, *J. Am. Chem. Soc.* **2008**, *130*, 16274-16286.

[18] a) J. S. Meisner, M. Kamenetska, M. Krikorian, M. L. Steigerwald, L. Venkataraman, C. Nuckolls, *Nano Lett.* **2011**, *11*, 1575-1579; b) S. Sangtarash, C. Huang, H. Sadeghi, G. Sorohhov, J. Hauser, T. Wandlowski, W. Hong, S. Decurtins, S.-X. Liu, C. J. Lambert, *J. Am. Chem. Soc.* **2015**, *137*, 11425-11431; c) E. Leary, C. Roche, H.-W. Jiang, I. Grace, M. T. González, G. Rubio-Bollinger, C. Romero-Muñiz, Y. Xiong, Q. Al-Galiby, M. Noori, M. A. Lebedeva, K. Porfyrakis, N. Agraït, A. Hodgson, S. J. Higgins, C. J. Lambert, H. L. Anderson, R. J. Nichols, *J. Am. Chem. Soc.* **2018**, *140*, 710-718; d) Z. Chen, L. Chen, J. Liu, R. Li, C. Tang, Y. Hua, L. Chen, J. Shi, Y. Yang, J. Liu, J. Zheng, L. Chen, J. Cao, H. Chen, H. Xia, W. Hong, *J. Phys. Chem. Lett.* **2019**, *10*, 3453-3458.

[19] D. Cabosart, M. El Abbassi, D. Stefani, R. Frisenda, M. Calame, H. S. J. van der Zant, M. L. Perrin, *Appl. Phys. Lett.* **2019**, *114*, 143102.

[20] a) M. S. Inkpen, Z.-F. Liu, H. Li, L. M. Campos, J. B. Neaton, L. Venkataraman, *Nat. Chem.* **2019**, *11*, 351-358; b) V. Sacchetti, J. Ramos-Soriano, B. M. Illescas, M. T. González, D. Li, L. Palomino-Ruiz, I. R. Márquez, E. Leary, G. Rubio-Bollinger, F. Pauly, N. Agraït, N. Martín, *J. Phys. Chem. C* **2019**, *23*, 29386-29393.

[21] a) A. Mishchenko, D. Vonlanthen, V. Meded, M. Bürkle, C. Li, I. V. Pobelov, A. Bagrets, J. K. Viljas, F. Pauly, F. Evers, M. Mayor, T. Wandlowski, *Nano Lett.* **2010**, *10*, 156-163; b) L. Venkatarman, J. E. Klare, C. Nuckolls, M. Hybertsen, M. L. Steigerwald, *Nature*, **2006**, *442*, 904-907.

[22] J. R. Quinn, F. W. Foss, L. Venkataraman, R. Breslow, *J. Am. Chem. Soc.* **2007**, *129*, 12376-12377.

[23] J. E. Anthony, *Angew. Chem. Int. Ed.* **2008**, *47*, 452-483; *Angew. Chem.* **2008**, *120*, 460-492.

[24] For selected examples of on-surface synthesis of higher acenes see: a) R. Zuzak, R. Dorel, M. Krawiec, B. Such, M. Kolmer, M. Szymonski, A. M. Echavarren, S. Godlewski, *ACS Nano* **2017**, *11*, 9321-9329; b) L. Colazzo, M. S. G. Mohammed, R. Dorel, P. Nita, C. García Fernández, P. Abufager, N. Lorente, A. M. Echavarren, D. G. De Oteyza, *Chem. Commun.* **2018**, *54*, 10260-10263; c) R. Zuzak, R. Dorel, M. Kolmer, M. Szymonski, S. Godlewski, A. M. Echavarren, *Angew. Chem. Int. Ed.* **2018**, *57*, 10500-10505; *Angew. Chem.* **2018**, *130*, 10660-10665; d) J. Krüger, F. Eisenhut, D. Skidin, T. Lehmann, D. A. Ryndyk, G. Cuniberti, F. García, J. M. Alonso, E. Guitián, D. Pérez, D. Peña, G. Trinquier, J.-P. Malrieu, F. Moresco, C. Joachim, *ACS Nano* **2018**, *12*, 8506-8511; e) J. I. Urgel, S. Mishra, H. Hayashi, J. Wilhelm, C. A. Pignedoli, M. Di Giovannantonio, R. Widmer, M. Yamashita, N. Hieda, P. Ruffieux, H. Yamada, R. Fassel, *Nat. Commun.* **2019**, *10*, 861; f) F. Eisenhut, T. Kühne, F. García, S. Fernández, E. Guitián, D. Pérez, G. Trinquier, G. Cuniberti, C. Joachim, D. Peña, F. Moresco, *ACS Nano* **2020**, *14*, 1011-1017. For examples of synthesis in solid state or solid matrix, see references cited in 23e.

[25] a) M. Bendikov, H. M. Duong, K. Starkey, K. N. Houk, E. A. Carter, F. Wudl, *J. Am. Chem. Soc.* **2004**, *126*, 7416-7417; b) K. J. Thorley, J. E. Anthony, *Isr. J. Chem.* **2014**, *54*, 642-649; c) Y. Yang, E. R. Davidson, W. Yang, *Proc. Natl. Acad. Sci. USA* **2016**, *113*, E5098-E5107; d) G. Trinquier, G. David, J. P. Malrieu, *J. Phys. Chem. A* **2018**, *122*, 6926-6933.

[26] a) T. Agou, J. Kobayashi, T. Kawashima, *Org. Lett.* **2006**, *8*, 2241-2244; b) A. Tomohiro, A. Hiroki, K. Takayuki, *Chem. Lett.* **2010**, *39*, 612-613; c) S. Madayanad Suresh, E. Duda, D. Hall, Z. Yao, S. Bagnich, A. M. Z. Slawin, H. Bässler, D. Beljonne, M. Buck, Y. Olivier, A. Köhler, E. Zysman-Colman, *J. Am. Chem. Soc.* **2020**, *142*, 6588-6599.

[27] T. Yelin, R. Korytár, N. Sukenik, R. Vardimon, B. Kumar, C. Nuckolls, F. Evers, O. Tal, *Nature Mater.* **2016**, *15*, 444-449.

[28] S. Wu, M. T. González, R. Huber, S. Grunder, M. Mayor, C. Schönenberger, M. Calame, *Nature Nanotech.* **2008**, *3*, 569–574.

[29] a) M. Brandbyge, J.-L. Mozos, P. Ordejón, J. Taylor, K. Stokbro, *Phys. Rev. B* **2002**, *65*, 165401; b) N. Papior, N. Lorente, T. Frederiksen, A. García, M. Brandbyge, *Comput. Phys. Commun.* **2017**, 212, 8-24.

[30] G. Kresse, J. Furthmüller, *Phys. Rev. B*, **1996**, *54*, 11169.

[31] a) D. J. Mowbray, G. Jones, K. S. Thygesen, *J. Chem. Phys.* **2008**, *128*, 111103; b) L. Zotti, M. Bürke, F. Pauly, W. Lee, K. Kim, W. Jeong, Y. Asal, P. Reddy, J. C. Cuevas, *New. J. Phys.* **2014**, *16*, 015004; c) T. Markussen, C. Jin, K. S. Tygesen, *Phys. Status Solidi B* **2013**, *250*, 2394-2402.

[32] a) T. Fu, S. Smith, M. Camarasa-Gómez, X. Yu, J. Xue, C. Nuckolls, F. Evers, L. Venkatamaran, S. Wei, *Chem. Sci.* **2019**, *10*, 9998-10002; b) Y. Kim, S. G. Bahoosh, D. Sysoiev, T. Huhn, F. Pauly, E. Scheer, *Beilstein J. Nanotechnol.* **2017**, *8*, 2606-2614.

[33] S. Guo, J. Hihath, I. Díez-Pérez, N. Tao, *J. Am. Chem. Soc.* **2011**, *133*, 19189-19197.

[34] M. Koepf, C. Koenigsmann, W. Ding, A. Batra, C. F. A. Negre, L. Venkataraman, G. W. Brudvig, V. S. Batista, C. A. Schmuttenmaer, R. H. Crabtree, *Nanoscale* **2016**, *8*, 16357-16362.

[35] a) G. P. Zhang, Z. Xie, Y. Song, M. Z. Wei, G. C. Hu, C. K. Wang, *Org. Electron.* **2017**, *48*, 29-34; b) S. Gil-Guerrero, N. Ramos-Berdullas, M. Mandado, *Org. Electron.* **2018**, *61*, 177-184.

[36] P. v. R. Schleyer, C. Maerker, A. Dransfel, H. Jiao, N. J. R. v E. Hommes, *J. Am. Chem. Soc.* **1996**, *118*, 6317-6318.

[37] a) R. G. Poranne, A. Stanger, *Chem. Eur. J.* **2014**, *20*, 5673-5688; b) A. Stanger, *J. Org. Chem.* **2010**, *75*, 2281-2288.

Entry for the Table of Contents

Insert graphic for Table of Contents here.

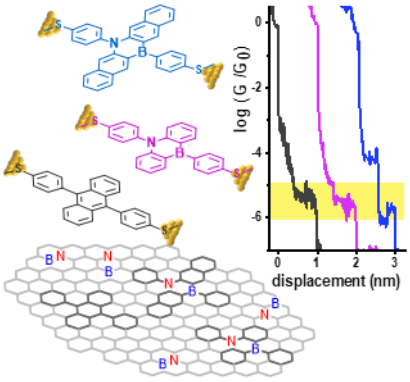

Insert text for Table of Contents here.

Single-molecule conductance of 1,4-azaborine acene type compounds studied using the scanning tunnelling microscope break-junction technique. This substitution ensures an unambiguous electron path through both heteroatoms. A moderate change in conductance is observed when compared to the parent all-carbon structure. State-of-the-art transport calculations support the experimental results.

Institute and/or researcher Twitter usernames: @MOR_Fun_Group; @Campana_Lab; @UEQuimica_ugr; @CanalUGR